Blood-brain barrier leakage in renovascular hypertensive rats: a quantitative MRI analysis

María Luz Alonso-Alonso , Ana Sampedro-Viana , Ivan Fernandez-Bueno , María Pérez-Mato , Clara Correa-Paz , Lara Pérez-Gayol , Daniel Romaus-Sanjurjo , Alberto Ouro , Javier Blanco-Santero , Crhistian-Mario Oblitas , José Castillo , Pablo Hervella , Ramón Iglesias-Rey

PII: S1053-8119(25)00286-1
DOI: https://doi.org/10.1016/j.neuroimage.2025.121283
Reference: YNIMG 121283

To appear in: *NeuroImage*

Received date: 18 December 2024
Revised date: 5 May 2025
Accepted date: 18 May 2025

Please cite this article as: María Luz Alonso-Alonso , Ana Sampedro-Viana , Ivan Fernandez-Bueno , María Pérez-Mato , Clara Correa-Paz , Lara Pérez-Gayol , Daniel Romaus-Sanjurjo , Alberto Ouro , Javier Blanco-Santero , Crhistian-Mario Oblitas , José Castillo , Pablo Hervella , Ramón Iglesias-Rey , Blood-brain barrier leakage in renovascular hypertensive rats: a quantitative MRI analysis, *NeuroImage* (2025), doi: https://doi.org/10.1016/j.neuroimage.2025.121283

Highlights

- Gadolinium-enhanced MRI allows *in vivo* blood-brain barrier (BBB) leakage assessment.
- Brain increment of aquaporin 4 supports BBB dysfunction secondary to hypertension
- Altered release of sTWEAK also supports BBB dysfunction secondary to hypertension.
- RHRSP are suitable for testing therapeutic/diagnostic tools in cSVD early stages.


Figure_1.eps

Blood-brain barrier leakage in renovascular hypertensive rats: a quantitative MRI analysis

Author information

María Luz Alonso-Alonso[a,*,1], Ana Sampedro-Viana[a,1], Ivan Fernandez-Bueno[b,c,*], María Pérez-Mato[d], Clara Correa-Paz[e], Lara Pérez-Gayol[d], Daniel Romaus-Sanjurjo[f,g], Alberto Ouro[f,g], Javier Blanco-Santero[b], Crhistian-Mario Oblitas[a], José Castillo[a], Pablo Hervella[a], Ramón Iglesias-Rey[a,*]

[a]Neuroimaging and Biotechnology Laboratory (NOBEL), Clinical Neurosciences Research Laboratory (LINC), Health Research Institute of Santiago de Compostela (IDIS), Santiago de Compostela, A Coruña, Spain

[b]Instituto Universitario de Oftalmobiología Aplicada (IOBA), Retina Group, Universidad de Valladolid, Valladolid, Spain.

[c]Departamento de Cirugía, Oftalmología, Otorrinolaringología y Fisioterapia, Facultad de Medicina, Universidad de Valladolid, Valladolid, Spain

[d]Translational Stroke Laboratory (TREAT), Clinical Neurosciences Research Laboratory (LINC), Health Research Institute of Santiago de Compostela (IDIS), Santiago de Compostela, A Coruña, Spain

[e]Neuroscience and Cerebrovascular Research Laboratory, Department of Neurology and Stroke Center, La Paz University Hospital, Neuroscience Area of IdiPAZ Health Research Institute, Universidad Autónoma de Madrid, Madrid, Spain.

[f]NeuroAging Laboratory Group (NEURAL), Clinical Neurosciences Research Laboratory (LINC), Health Research Institute of Santiago de Compostela (IDIS), Santiago de Compostela, A Coruña, Spain

[g]Centro de investigación Biomédica en Red de Enfermedades Neurodegenerativas, Instituto de Salud Carlos III, Madrid, Spain

1 These authors contributed equally to this work.

Corresponding authors

Ramón Iglesias-Rey: Health Research Institute of Santiago de Compostela (IDIS), Clinical University Hospital (CHUS), Travesía da Choupana, s/n, Santiago de Compostela. E15706 A Coruña, Spain. Email: ramon.iglesias.rey@sergas.es

Ivan Fernandez-Bueno: Instituto Universitario de Oftalmobiología Aplicada (IOBA), Paseo de Belén, 17, 47011 Valladolid, Spain. Email: ivan.fernandez.bueno@uva.es

María Luz Alonso-Alonso: Health Research Institute of Santiago de Compostela (IDIS), Clinical University Hospital (CHUS), Travesía da Choupana, s/n, Santiago de Compostela. E15706 A Coruña, Spain. Email: maria.luz.alonso.alonso@sergas.es

Abstract

Hypertension is a modifiable risk factor for cerebral small vessel disease (cSVD) which leads to blood-brain barrier (BBB) dysfunction. This study used gadolinium-enhanced MRI T_1 and T_2 in stroke-prone renovascular hypertensive rats (RHRSP) to quantify BBB leakage and brain lesions. Serum inflammation and endothelial disruption biomarkers were assessed. Brain aquaporin 4 (AQ4) and retinal morphology were evaluated by histology. RHRSP showed higher systolic blood pressure from the first post-surgical week (134.1 ± 16.6 vs 113.5 ± 11.4 mmHg; p=0.041). Gadolinium extravasation was increased in the whole brain of RHRSP (p<0.05), observing cerebral lesions in 50% of them. Regarding biomarkers, TNF-α was increased (13.5 ± 2.2 vs 11.1 ± 3.5 pg/ml, p=0.031) while soluble tumor necrosis factor-like weak inducer of apoptosis (sTWEAK) was lower (14.5 ± 2.2 vs 18.9 ± 2.5 pg/ml, p<0.001) in the acute hypertension phase. AQ4 was increased in the RHRSP brain (1.6 ± 0.7 vs 1.0 ± 0.2 NFU; p=0.001). Both retinal nuclear layers were reduced in RHRSP (p<0.05). Gadolinium-enhanced MRI allows the detection of BBB leakage during the establishment of RHRSP. BBB dysfunction is consistent with increased AQ4 and decreased sTWEAK release. Therefore, this animal model is useful for testing potential treatments at cSVD initial stages.

Keywords

Blood–brain barrier; Gadolinium; Magnetic resonance imaging; Small vessel disease; Stroke-prone renovascular hypertensive rats (RHRSP)

1. Introduction

In recent decades, the number of people with hypertension has doubled, although the global prevalence in adults (32% in women vs 34% in men) remains stable due to the different trends in high, middle, and low-income countries (NCD Risk Factor Collaboration (NCD-RisC)., 2021). Hypertension is one of the main modifiable risk factors not only for cardiovascular but also cerebrovascular diseases (Boehme et al., 2017; Castillo et al., 2004; Fuchs and Whelton, 2020; Leira et al., 2009), including cerebral small vessel disease (cSVD) (Cannistraro et al., 2019; Meissner, 2016; Wei et al., 2024). In the pathogenesis of cSVD, hypertension leads to the damage of cerebral vasculature, including endothelial cell injury and blood-brain barrier (BBB) dysfunction (Meissner, 2016; Wei et al., 2024). cSVD is involved in the most hemorrhagic strokes, in about a quarter of ischemic strokes, and vascular dementia (Wardlaw et al., 2019). Currently, this disease has limited therapeutic options, so advancing research in this field is essential (Markus and de Leeuw, 2023).

In this sense, several animal models have been widely used to study cSVD. According to the type of model, they can be classified as embolic models, hypoperfusion (or ischemic injury), vessel damage, and hypertension-based injury (Hainsworth and Markus, 2008). Considering the role played by hypertension in the cSDV (Cannistraro et al., 2019; Meissner, 2016; Wei et al., 2024), the last type of model could be appropriated to resemble human disease. Previously, Okamoto et al. (1974) had characterized the stroke-prone spontaneously hypertensive rat (SHRSP). The SHRSP animal model developed hypertension spontaneously and between 60-80% of them suffer from cerebral lesions (Okamoto et al., 1974). Although the SHRSP model has been used

broadly leading to relevant advances in this field (Bailey et al., 2011; Hainsworth and Markus, 2008), the unknown potential interference of genetic alteration with study results (Nabika et al., 2004) and the elevated price of this strain are limitations to be considered. On the other hand, the stroke-prone renovascular hypertensive rat (RHRSP) model was described by Zeng et al. (1998). The RHRSP animal model developed hypertension after placing a clip on each renal artery and showed a 61.8% incidence of stroke (Zeng et al., 1998) preventing the influence of genetic factors. This fact, along with its reduced cost, makes RHRSP an affordable alternative model for testing new diagnosis tools and potential treatment

Since the magnetic resonance image (MRI) is an essential tool for the diagnosis of cSVD (Duering et al., 2023), previous studies in the RHRSP model have shown white-matter hyperintensities, a small focus on acute hemorrhage, ischemic infarcts, and reduced cerebral blood flow. Furthermore, chronic hypertension induces vascular remodeling, endothelial dysfunction, and BBB permeability (Elsaid et al., 2021). However, to our knowledge, no data is reported about the evaluation of BBB by MRI in the RHRSP rats, although the endothelium damage and the dysfunction of BBB seem to be critical factors in the pathogenesis of cSVD (Hannawi, 2024; Ihara and Yamamoto, 2016).

On the other and, hypertension not only affects brain vessels, but also those placed in the retina (Dziedziak et al., 2022), being hypertensive retinopathy associated with a higher risk of stroke (Ong et al., 2013). Based on these facts, we hypothesized that RHRSP rats could develop retinal alterations as early biomarkers associated with stroke risk. Similarly, blood biomarkers are widely used for additional information to stablishing a prognosis in stroke (Montellano et al., 2021). Therefore, measuring indirect

biomarkers of endothelial dysfunction in hypertensive rats could be a key point for using this animal model in personalized medicine research.

In the present study, we studied the BBB leakage by MRI (T_1-weighted image) during the establishment of a hypertensive status in the RHRSP rats. This animal model could be useful for detecting early BBB disruption due to chronic hypertension, and therefore, an appropriate model for testing new tools for early diagnosis and potential therapeutic options for initial stages of the disease. The secondary endpoints were to determine the assessment of blood biomarkers of renal function, inflammation and endothelial dysfunction. Additionally, the retinal general morphology was evaluated as a potential biomarker of early alteration of the central nervous system secondary to hypertension.

2. Material and methods

2.1. Animals and study design

The use of animals in this study was approved by the Animal Research and Welfare Ethics Committee of the Health Research Institute of Santiago de Compostela (IDIS; Santiago de Compostela, Spain) and was authorized under procedure number 15011/2021/002 by the Farming and Ranching Agency of Xunta de Galicia (Regional Government, Spain) in agreement with European (Council Directive 2010/63/UE) and Spanish regulations (RD 53/2013). The studies followed the ARRIVE guidelines (Animal Research: Reporting in Vivo Experiments).

Twelve (n=12) male Sprague–Dawley rats [4 weeks old, 113±15 g; Experimental Biomedicine Centre (CEBEGA) of the University of Santiago de Compostela] were used. The animals were randomly divided into sham (normotensive, n=6) and hypertension (hypertensive, n=6) groups. Online software (Experimental Design Assistant;

https://eda.nc3rs.org.uk/eda/login/auth) was used for the sample size calculation and the animal randomization. The sample size of this study was calculated based on the variance obtained from pilot study using this animal model (SD=14), a significance level of 0.05 and a power of 90%. The animals were included in the study if they underwent successful hypertension, defined as systolic BP > 150 mmHG 3 weeks post-surgery. The animals were excluded if a vessel was damaged during the surgery. The rats were housed in pairs in cages with enriched cardboard material. Animals were kept in a controlled environment at 22°C ± 1°C and 60% ± 5% humidity, with 12:12 h light:darkness cycles, and had free access to standard food and water for a week before surgical procedure and up to 20 weeks after surgical procedure.

2.2. Surgical procedure to induce hypertension

The induction of the RHRSP model was performed using the method of two-kidney, two-clip (2k2c) previously described by Zeng et al. (1998). Analgesia was applied by subcutaneous injection of meloxicam (1.5-2 mg/kg; Metacam, 2mg/ml, Boehringer Ingelheim Vetmedica GmbH, Ingelheim am Rhein, Germany). Rats were anesthetized using isoflurane at 2-3% (Abbott Laboratories, IL, USA) using a carrier 70:30 gas mixture of N_2O: O_2 and underwent a lateral incision on the right abdominal skin. The right renal artery was exposed and ring-shaped Luminy® Polylactic acid (PLA) polymer stenosis clips (0.30-0.35 mm inner diameter, LEON3D, León, Spain) were placed around the roots of the artery (Fig. 1S). The same procedure was performed in the left renal artery. The sham-operated group received the same surgical procedure without placing the renal artery clips.

2.3. Blood pressure measurement

Systolic and diastolic BP was measured by an indirect tail-cuff method (Panlab non-invasive blood pressure system, Panlab Harvard Apparatus, Barcelona, Spain) in conscious rats previously and weekly after renal arteries stenosis. Rats were previously accustomed to the holder and the tail-cuff to minimize high BP secondary to stress. BP measurements were collected by the same researcher in the mornings under the same environmental conditions.

2.4. Magnetic resonance imaging

All MRI studies were conducted on a Bruker Biospec 9.4 T MR (Bruker, Billerica, MA, USA) scanner (horizontal bore magnet with 12 cm wide Bruker BioSpin) equipped with actively shielded gradients (440 mT m^{-1}). Animals were imaged with a combination of a linear birdcage resonator (7 cm in diameter) for signal transmission and a 2×2 surface coil array for signal detection, positioned over the head of the animal, which was fixed with a teeth bar, earplugs, and adhesive tape. Transmission and reception coils were actively decoupled from each other. Animals were anesthetized with sevoflurane at 3–4% (Abbott Laboratories, IL, USA) and respiratory frequency and body temperature were monitored throughout the experiment.

A T_1-weighted gadolinium-enhanced MRI (Gd; Dotagraf 0.5 mmol/ml; Bayer Hispania, Barcelona, Spain) was performed before and every two weeks after hypertensive induction. T_1-weighted MR images (Rapid Acquisition with Relaxation Enhancement sequence (RARE)) with an echo time (ET)= 7.5 ms, rare factor (RF)= 2, 6 T_1 experiments with repetition time (RT) = 540, 800, 1000, 1500, 3000, and 6000 ms, 1 average, spectral bandwidth (SW)= 90 KHz, 19 consecutive slices of 1 mm, 19.2 × 19.2 mm^2 field of view

(FOV) with saturation bands to suppress signal outside this FOV, a matrix size of 128 × 128 (isotropic in-plane resolution of 150 µm/pixel × 150 µm/pixel) and implemented without fat suppression option.

For T_2 map calculated from a T_2-weighted image, a multi-slice multi-echo (MSME) sequence: ET = 9 ms, RT = 3 s, 16 echoes with 9 ms echo spacing, flip angle = 180º, NA = 2, SW = 75 KHz, 20 slices of 1 mm, 19.2 × 19.2 mm^2 FOV (with saturation bands to suppress signals outside this FOV), a matrix size of 192 × 192 (isotropic in-plane resolution of 100 µm/pixel × 100 µm/pixel), and implemented without the fat suppression option.

2.5. MRI analysis

Regional Gd-leakage maps were calculated to analyze the BBB extravasation of Gd following the protocol described by van Vliet et al. (2014) in the whole brain, cortex, corpus callosum, striatum, and hippocampus. Briefly, Gd (0.2 M diluted in saline) was injected via the tail vein using a syringe pump (Harvard Apparatus, Holliston, MA, USA) programmed to dispense it according to the infusion schedule of Table 1S. T_1-weighted images were conducted before and immediately after the 20-minute step-down infusion. Gd-leakage was calculated as the relative signal enhancement induced by Gd accumulation. The regional leakage maps were thresholded at 0.2, similarly as described previously (van Vliet et al., 2014). For each animal, a Gd leakage map was created by digitally subtracting the pre-contrast T_1-weighted signal intensity from the post-contrast signal intensity and dividing by the pre-contrast signal intensity, using the corresponding T_1 maps, as previously described (van Vliet et al., 2016, 2014).

A T_2 map calculated from a T_2-weighted image was performed weekly after hypertensive induction to evaluate morphological brain alterations and measure volume changes in the same brain regions. Additionally, T_2-weighted images, averaged from echoes 4 to 8 of the MSME sequence, were used to aid in visualizing potential brain lesions. To prevent gadolinium-affected T_2 study due to its time of clearance in the brain, in those weeks in which the rats underwent both MRI studies, the T_2-weighted image was performed before the T_1 gadolinium-enhanced images in all cases. Images were processed using ImageJ (Rasband WS, National Institutes of Health, Bethesda, MD, USA, http://rsb.info.nih.gov/ij/) on an independent computer workstation by a researcher blinded to the animal protocols.

2.6. Analysis of blood biomarkers

Blood samples were collected from the jugular vein before hypertension induction and from the tail vein weekly after the surgery. The samples were collected into SST™ blood collection tubes (BD Microtainer, Franklin Lakes NJ, USA) and centrifuged at 1700× g for 7 min, and storing serum at −80 ◦C until analysis. Serum levels of interleukin-1 Beta (IL-1β), IL-2, IL-6, IL-10 and tumor necrosis factor alpha (TNF-α) were determined using a customized Milliplex MAP Rat Cytokine/Chemokine Magnetic Bead Panel kit for these selected molecules (Cat. RECYTMAG-65K, EMD Millipore, Darmstadt, Germany). The analysis was performed according to manufacturer's guide and the beads were detected using Bio-Plex 200 System with the software Bio-Plex Manager Software, v. 6.2 Build 175 (Bio-Rad, Hercules, Ca, USA). Similarly, ELISA kits were performed to measure matrix metalloproteinase-9 (MMP9; Quantikine® ELISA Rat Total MMP-9 Immunoassay, Cat. RMP900, R&D Systems Europe, Minneapolis, MN, USA) and soluble tumor necrosis

factor-like weak inducer of apoptosis (sTWEAK; Rat TNFSF12 ELISA kit, Cat. ab213915, abcam) in serum. Additionally, urea and creatinine levels, as renal function markers, were measured with Reflotron®plus (Roche, Vienna, Austria) by adding 32 µL of a blood sample to reactive strips (Cat. 11200666 and Cat. 10886874 respectively, Roche).

2.7. Tissue processing

Humane endpoints were applied in two animals of RHRSP group at weeks 17 and 19 post-surgery. The rest animals were sacrificed at week 20 post-surgery by an overdose of anesthesia, and then transcardially perfused with an ice-cold solution of phosphate-buffered saline (PBS) followed by 4% paraformaldehyde (PFA). The brains and eyes were dissected out, and the tissues were post-fixed overnight at 4°C in the same fixative solution.

OCT blocks from each brain were prepared and then transversely sectioned with a cryostat at a thickness of 14 µm. For immunohistochemistry, the sections were rinsed with PBS, permeabilized (1% triton) and blocked (bovine serum albumin 5%) for 30 minutes and 1 hour respectively. Incubation in the primary antibody aquaporin 4 (AQ4, 1:500; Cat. ab9512, abcam; Cambridge, UK) was carried out at 4°C overnight. Then, slides were washed in PBS and corresponding species-specific secondary antibodies conjugated to Alexa Fluor 647 (ab150119; 1:1000; abcam) were added and incubated for 1.5 hours at RT in the dark. After that, nuclei were counterstained with Hoechst 33342 for 10 min, mounted with Aqua-Poly/Mount (Polysciences, Warrington, PA, USA), and coverslipped. Control samples in which the primary antibodies were omitted, were processed in parallel and no immunoreactivity was found in any case. Micrographs on magnification ×10 were taken with a confocal microscope (Leica TCS SP8, Leica

Microsystems, Wetzlar, Germany). Immunoreactivity semi-quantification was measured in the brain using Fiji software (Schindelin et al., 2012).

For the processing of the eyeballs and evaluation of the retinas, we have followed protocols previously described (Fernandez-Bueno et al., 2019, 2017). One paraffin block of each eye was made and vertical serial 4-µm thick sections through the optic disc were obtained in a rotatory microtome. Then, ocular sections were de-waxed in xylene, rehydrated in a series of descending alcohols (100°, 96°, and 80°), rinsed in deionized distilled water, and stained with hematoxylin and eosin (HE; Merck KGaA, Darmstadt, Germany). Stained sections were finally dehydrated in a series of ascending alcohols (96° and 100°), cleared in xylene, mounted, and coverslipped. Manual nuclei cell counting, at outer and inner nuclear layers (ONL and INL; nuclei in a stack), was performed on magnification ×40 micrographs derived from non-serial HE neuroretina sections, using the ImageJ software.

2.8. Statistical analyses

A researcher blinded to the animal group analyzed data. All animals were included in the study since all showed the BP expected. All data were collected in a database created in Excel (Microsoft Office Excel 2016; Microsoft Corporation, Redmond, WA, USA) and subsequently analyzed by SPSS software (IBM® SPSS® Statistics for Windows v20, SPSS Inc. Armonk, NY, USA). The data of both MRI T1 and T2 were normalized to the mean of basal and first week mean of each group, respective, before analyzing. Values were expressed as mean ± standard deviation (SD) and a p-value <0.05 was considered statistically significant in all analyses. The normality of the data was determined by Shapiro–Wilk normality. A comparison of means in each experiment was performed

using the Mann-Whitney U test. Graphs were made using GraphPad Software (GraphPad Prism V.8.0.1, Boston, MA, USA).

3. Results

3.1. Mortality rate and blood pressure

Two rats were euthanized as a humane endpoint in the RHRSP group in weeks 16 and 19 respectively during the study. No rat died in the sham group throughout the experiment. Regarding BP, no significant difference was observed in basal systolic or diastolic BP between sham and RHRSP groups (102.7 ± 6.6 vs 99.5 ± 8.8 mmHg; 76.0 ± 13.5 vs 77.6 ± 8.5 mmHg respectively). Systolic BP was significantly higher in the RHRSP group since the first post-surgical week (134.1 ± 16.6 vs 113.5 ± 11.4 mmHg; p = 0.041; Fig. 1A). This significant increment was observed in diastolic BP since the second week post-surgery (118.5 ± 11.2 vs 98.9 ± 14.2 mmHg; p=0.026; Fig. 1B). According to these results, the hypertension was divided into two phases, acute hypertension (weeks 1-12) and chronic hypertension (weeks 13-20).

3.2. MRI analysis: cerebral alterations and brain blood-barrier leakage

MRI were normalized to the baseline value of each group for both T_1 and T_2 maps. The T_2 maps showed a significant reduction in signal values in the RHRSP group in weeks 5 and 10 after hypertension induction in the whole brain, cortex, corpus callosum, and striatum (Fig. 2A-E). In the corpus callosum, this reduction was also observed in week 15, while in the hippocampus it was only significant in week 5 post-surgery. No differences were observed in these region volumes, except in the hippocampus where the RHRSP group showed a significant increment (Fig. S2). Regarding brain injury, 3 of the 6 RHRSP rats showed cerebral ischemic lesions, 2 of them in the lateral ventricle and

the other in cortex and lateral hypothalamus (Table S2). Only one of these rats showed cerebral hemorrhage, which was located in the lateral hypothalamus (Fig. 2F). Finally, T_1 maps showed an increase in BBB leaked measured by gadolinium extravasation into the whole brain and striatum of RHRSP rats in 4, 10, and 16 weeks after surgery (Fig. 3A, B and E). In the hippocampus, this extravasation was only significant in week 10 post-surgery (Fig. 3F). Unexpectedly, the gadolinium extravasation was lower in the RHRSP group in the cortex in weeks 16 and 20 and corpus callosum in the week 20 (Fig. 3C-D).

3.3. Blood biomarkers of renal function, inflammation, and endothelial disruption

We have observed a significant increment of both biomarkers of renal function, urea (40.7 ± 7.2 vs 33.8 ± 3.4 mg/dl; 39.9 ±3.9 vs 33.6 ± 5.0 vs mg/dl $p<0.001$; acute and chronic hypertension respectively, Fig. 4A) and creatinine (0.52 ± 0.02 vs < 0.500 mg/dl; 0.58 ± 0.13 vs 0.501 ± 0.003 mg/dl, $p<0.001$; acute and chronic hypertension respectively, Fig. 4B) post-surgery. Regarding inflammatory biomarkers, it only showed a significant increase in TNF-α in the acute hypertension phase of the RHRSP group (13.5 ± 2.2 vs 11.1 ± 3.5 pg/ml, $p=0.031$, but not in the chronic hypertension phase (Fig. 4C) nor IL-1β, IL-2, and IL-10 (Fig. S3 A-C). Finally, sTWEAK and MMP9 were analyzed as indirect endothelial disruption biomarkers. The sTWEAK serum levels were significantly lower in the RHRSP than the sham group during the acute hypertension phase (14.5 ± 2.2 vs 18.9 ± 2.5 pg/ml, $p<0.001$, Fig. 4D). However, there were no differences during the chronic hypertension phase. Finally, no differences were observed in the MMP9 serum levels (Fig. S3D).

3.4. Increment of aquaporin 4 as response to excessive fluid entering in brain

As shown in Fig. 5A-B, AQP4 immunostaining brain sections showed that protein levels were significantly increased in the RHRSP group compared to the sham group (1.6 ± 0.7 vs 1.0 ± 0.2 Normalized Fluorescence Units (NFU); p=0.001; Fig. 6C), supporting the BBB dysfunction secondary to chronic blood hypertension.

3.5. Retinal alterations secondary to hypertension

The general morphology of the retinas from sham and RHRSP animals was normal in appearance. Retinas showed the typical highly organized layered structure with cells regularly arranged (Fig. 6 A-B). Photoreceptor outer and inner segments and the outer nuclear layer (ONL), inner nuclear layer (INL), and ganglion cell layers were easily recognized. However, the total mean number of nuclei in a stack in the ONL and INL was significantly reduced ($p<0.05$) in the RHRSP rats (8.4 ± 0.5 and 3.6 ± 0.7) when compared with the sham ones (10.6 ± 0.5 and 4.4 ± 0.5) (Fig. 6C).

4. Discussion

In this study, we analyzed for the first time the BBB leakage throughout the establishment of the hypertensive state in RHRSP model by MRI. We found that the extravasation of gadolinium was increased in the whole brain hypertensive rats which appears to reveal a dysfunction of the BBB since the early increment of blood pressure. This hypothesis is also supported by the increment of expression of the protein AQP4 in RHRSP. Although the pathophysiology of cSVD is not completely understood, the dysfunction of BBB seems to play an essential role in it (Hainsworth et al., 2024; Ihara and Yamamoto, 2016; Wardlaw et al., 2019). On the other hand, MRI is widely used in clinical practice for its diagnosis (Duering et al., 2023; Markus and de Leeuw, 2023). Therefore, characterizing the RHRSP animal model in terms of BBB leakage using MRI

would be useful for testing not only new tools for early diagnosis but also potential therapeutic options.

Hypertension is considered the first modifiable risk of cerebrovascular diseases, including cSVD (Boehme et al., 2017; Meschia et al., 2014; Wajngarten and Silva, 2019). Thus, several animal models of systemic hypertension have been extensively used as animal models of cSVD (Hainsworth and Markus, 2008; Mustapha et al., 2019; Shindo et al., 2020), being one of the most selected in this field the SHSP rats. However, the unknown influence of their genetic alteration on the results is a limitation of this animal model that should be noted (Nabika et al., 2004). On the other hand, RHRSP rats become hypertensive by surgical reduction of blood flow in both renal arteries (Zeng et al., 1998). Therefore, this approach allows the development of a similar animal model avoiding the potential influence of genetic factors which could involve an additional difficulty in the transference of results to clinical practice in long term. However, the researchers who use this animal model use silver clips (Chen et al., 2014; Lin et al., 2017a; Liu et al., 2007; Zhang et al., 2020) that are not commercialized, preventing this animal model from being selected by other researchers. Thus, we designed new clips for 3D printing in the present study. The design was based on the clips described by Park et al. (Park et al., 2016) to induce stenosis in the abdominal aorta in rats while maintaining the inner diameter of 0.3 mm used for this model (Chen et al., 2014; Lin et al., 2017a; Liu et al., 2007; Zeng et al., 1998). Following this protocol, 100% of rats in the hypertensive group showed SBP > 150 mmHG at 3 weeks post-surgery. Similar to it previously described (Chen et al., 2014; Li et al., 2015; Ling et al., 2009), SBP became steady at 12 weeks post-surgery in our RHRSP rats. Based on these facts, the hypertension progression was divided into two phases, acute (weeks 1-12) and chronic hypertension (weeks 13-20).

Regarding the neuroimaging study, the alteration of the T_2 signal was lower in hypertensive rats, which was statistically significant only during the acute hypertensive phase for the whole brain, cortex, striatum, and hippocampus, and also at week 15 in the corpus callosum. Thus, a trend was observed to be lower during the weeks when SBP was increasing. The reduction of relaxation time of T_2 has been proposed as a noninvasive detection method of cerebral hypoperfusion (Gröhn et al., 1998). Additionally, an MRI perfusion study in RHRSP rats concluded they develop cerebral hypoperfusion in the early phase of hypertension (Xu et al., 2024), which supports our results.

Concerning brain volume, it was observed a significant increment in the hippocampus of hypertensive rats. An increase in hippocampal volume in hypertensive patients is not commonly observed and would be unusual given the established research that links hypertension to hippocampal atrophy. However, if such a finding is reported, there could be several potential explanations or hypotheses to explore, such as early-stage hypertension, neuroplasticity or inflammation response.

Brain injuries were detected in T_2 images in 3 of the 6 RHRSP rats. This is slightly lower than previously described for this model (Del Bigio et al., 1999). This may be due to the difference in sample sizes in each study according to its objectives. However, cerebral ischemia seems to be the most frequent brain lesion (Zeng et al., 1998) which supports our findings.

White matter lesions (WML), visualised as hyperintensities on MRI (Fan et al., 2015a; Xu et al., 2024), indicate abnormal myelination in the brain and are considered one of the manifestations of cSVD, as well as a risk factor for severe cerebrovascular disease

(Duering et al., 2023; O'Sullivan, 2008). In our study, this alteration was not observed in the T_2 images. Xu et al. (2024) only observed WML in T_2 in 3 to 8 RHRSP at 20 weeks post-surgery, although it was detected postmortem in some of them with no T_2 hyperintensities. The severity of WML in RHRSP seems to increase with the duration of hypertension (Fan et al., 2015b), being mild before 12 weeks and becoming severe after 20 weeks (Fan et al., 2015a). However, the mortality rate in the last weeks of follow-up is a notable limitation for MRI studies of WML in RHRSP.

The dysfunction of BBB is claimed to be involved in the pathogenies of WML (Huang et al., 2018; Lin et al., 2017b; Simpson et al., 2010), therefore it is possible to detect BBB increase of permeability by MRI previously than WM hyperintensities. Gadolinium-enhanced MRI has been widely used to evaluate BBB permeability in animal models of cerebral ischemia (Durukan et al., 2009; Morgan et al., 2020; Strbian et al., 2008), epilepsy (van Vliet et al., 2014), traumatic brain injury (van Vliet et al., 2020) and brain tumor (On et al., 2013). To the best of our knowledge, this is the first time that this MRI technique has been used for longitudinal *in vivo* assessment of BBB leakage in RHRSP rats. Our results showed a significant increase in gadolinium leakage in RHRSP group between weeks 4 and 16 post-surgery. The BBB dysfunction had been confirmed postmortem by leakage of albumin or tight junction disruption observed by transmission electron microscope (Del Bigio et al., 1999; Fan et al., 2015a, 2015b; Lin et al., 2017a). These observations support our outcome and reinforce the utility of gadolinium-enhanced MRI as a noninvasive tool for BBB assessment, reducing the sample size needed for these studies. Nevertheless, we observed a decrease compared to the sham group at the end of the study. We speculated that this finding could be a consequence of the adaptation and remodeling of BBB components to chronic hypertension that

might compensate for its permeability. The protective effect of adaptive changes in the BBB components has been proposed as the reason for the greater resistance of the BBB to acute hypertension in chronically hypertensive animals (Mueller and Heistad, 1980). Previous studies had described an increased number of pericytes in spontaneously hypertensive rats compared to normotensive ones (Herman and Jacobson, 1988), which plays an essential role in BBB permeability regulation (Armulik et al., 2010), also supports our hypothesis.

On the other hand, the cytokine TWEAK and its receptor fibroblast growth factor-inducible 14 (Fn14) are involved in the regulation of permeability of BBB (Yepes, 2013, 2007). The TWEAK seems to be expressed mainly in endothelial cells while Fn14 is expressed at a high level in perivascular astrocytes and neurons (Yepes, 2013). The soluble form of this cytokine (sTWEAK) is widely used as a biomarker of cerebrovascular and cardiovascular diseases (Blanco-Colio et al., 2007; Chorianopoulos et al., 2010; Comertpay et al., 2020; Dai et al., 2020; Hervella et al., 2024, 2021; Iglesias-Rey et al., 2022). The increase in TNF-α is also common in these patients (Dunlay et al., 2008; Xue et al., 2022). Thus, we have observed a significant elevation of TNF-α levels in the acute hypertension phase, which agrees with a previous study in this animal model (Lan et al., 2015). However, the RHRSP group showed lower levels of sTWEAK compared to the sham group during the increase of SBP. Although this result was unexpected, the diminution of this cytokine has been observed in chronic stable heart failure and atherosclerosis (Chorianopoulos et al., 2009; Fernández-Laso et al., 2015; Martín-Ventura et al., 2010). Additionally, smoking, a habit associated with vascular endothelial dysfunction (Higashi, 2023), also showed lower levels of sTWEAK (Iglesias-Rey et al.,

2022). Since TWEAK is expressed majority in the endothelium of the BBB (Yepes, 2013), increasing blood pressure could alter the normal release of sTWEAK.

BBB leakage secondary to hypertension also involve an excessive fluid entering the brain parenchyma, leading to an elevation of AQP4 levels to facilitate its reabsorption as response, decreasing brain pressure and potential tissue injury (Fukuda and Badaut, 2012). AQPs are a family of membrane proteins, widely distributed in the different tissues of the organism, which form channels to transport water across the cytoplasmic membrane (Verkman, 2013). In mammalian brain tissue, AQPs1, 4 and 9 are mainly expressed, being AQP4 the most abundant in the brain (Mader and Brimberg, 2019). A previous study had shown that SHRSP rats with chronic hypertension and leakage of the BBB, but without ischemia or hemorrhage, presented edema in the brain (Tamaki et al., 1984). Thus, the overexpression of AQP 1 and 4 was described in SHR rats. Our results confirmed the increased level of this AQP4 in the RHRSP group, which agrees with the increase of AQP4 reported in SHR rats (Tomassoni et al., 2010), and supports BBB dysfunction secondary to chronic blood hypertension. However, this edema was not reflected in a brain volume increment.

Finally, we evaluated the morphological changes in the retina as potential early biomarker of cerebral alteration. Hypertensive retinopathy is associated with a higher risk of stroke, even in treated patients with controlled hypertension (Ong et al., 2013). Indeed, it is commonly described in retinal alterations in stroke patients (Liang et al., 2022; Rodríguez et al., 2010; Wu et al., 2017) and retinal imaging has been suggested as a potential stroke risk biomarker (Girach et al., 2024). In the retina of hypertensive rats has been reported a narrowing of retinal vessel diameter, thinner ONL, and reduction of

cell density in this layer (Li et al., 2020). Thus, we hypothesized that RHRSP rats could develop retinal alterations which could be early biomarkers associated with stroke risk. A significant reduction in the number of nuclei of both the ONL and INL was detected after 20 weeks of hypertensive state, which is compatible with a reduction in the thickness of these layers. This result does support the use of this animal model for hypertensive retinopathy.

There are some limitations to our study. First, we only included males, and therefore the potential differences secondary to sex were not contemplated. However, the articles that used this animal model had only used males. Second, the RHRSP rats showed a high mortality rate, which limits the follow-up period for MRI studies. This fact introduces variability secondary to individual differences between groups. Third, assessing retinal alterations secondary to hypertension by histology at the end of follow-up, rather than retinal imaging by OCT or fundus fluorescein angiography, limits the information obtained about retinal changes occurring throughout the establishment of hypertension, and thus fully assessing its potential as an early biomarker. Fourth, although gadolinium-enhanced MRI is a well-established method for evaluating BBB permeability, incorporating Ktrans (volume transfer constant) measurements in future studies could provide additional insights and further validate BBB dysfunction results (Chaganti et al., 2023; Ying et al., 2024). Fifth, the gadolinium-enhanced MRI study only allows to analysis the paracellular (between cells) leakage of BBB but not the transcellular (across cells) one. Finally, due to the number of animals included in this study, the data did not follow a normal distribution, according to the Shapiro–Wilk normality test performed. Therefore, although a repeated measures ANOVA

(parametric test) would be the most appropriate test for this type of experimental design, the Mann-Whitney U test (non-parametric test) was selected in this case.

In conclusion, this study shows that BBB leakage throughout the establishment of the hypertensive state in RHRSP rats can be detected by gadolinium-enhanced MRI. The increase of AQ4 detected in the brain and the alteration of the release of sTWEAK by the endothelium also supports BBB dysfunction secondary to chronic blood hypertension in this animal model. Therefore, this animal model is useful for detecting early BBB disruption secondary to chronic hypertension, being an appropriate model for testing new diagnostic tools and potential therapeutic options for the initial stages of the disease. Future studies to establish the potential correlation between BBB leakage detected by gadolinium-enhanced MRI and other serum biomarkers BBB dysfunction in RHRSP model should be performed.

Data Availability

Data will be made available on request.

Funding

This work was supported by Spanish Ministry of Science and Innovation [SAF2017-84267-R, PDC2021-121455-I00], Xunta de Galicia [Consellería de Educación: IN607A2022-03], Instituto de Salud Carlos III (ISCIII) Co-financed by the European Union [PI21/01256], Spanish Research Network on Cerebrovascular Diseases RETICS-INVICTUS PLUS [RD16/0019/0001], RICORS-ICTUS (Cerebrovascular diseases) RD21/0006/0003. Ramón Iglesias-Rey [CP22/00061] from the Miguel Servet Program of Instituto de Salud Carlos III and Co-financed by the EU. Clara Correa-Paz [CD23/00005] from the Sara Borrell contract. Daniel Romaus-Sanjurjo [101066444] from the European Union's Horizon 2020 research and innovation program under the Marie Skłodowska-Curie grant Program. Sponsors did not participate in the study design, collection, analysis, or interpretation of the data, or in writing the report.

CRediT authorship contribution statemens

María Luz Alonso-Alonso: Methodology, Investigation, Formal analysis, Writing - Original Draft. **Ana Sampedro-Viana:** Methodology, Investigation, Formal analysis, Writing - Original Draft. **Ivan Fernandez-Bueno:** Methodology, Investigation. **María Pérez-Mato:** Investigation. **Clara Correa-Paz:** Investigation. **Lara Pérez-Gayol:** Investigation. **Daniel Romaus-Sanjurjo**: Writing - Review & Editing. **Alberto Ouro:** Writing - Review & Editing. **Javier Blanco-Santero:** Investigation. **Crhistian-Mario Oblitas:** Writing - Review & Editing, **José Castillo:** Conceptualization, Writing - Review & Editing, Supervision. **Pablo Hervella:** Conceptualization, Writing - Review & Editing.

Ramón Iglesias-Rey: Conceptualization, Methodology, Investigation, Formal analysis, Writing - Review & Editing, Supervision. All authors read, reviewed, and agreed on the manuscript version.

Declaration of conflict of interests

All authors declare no conflict of interest.

Ethical considerations

The use of animals in this study was approved by the Animal Research and Welfare Ethics Committee of the Health Research Institute of Santiago de Compostela (IDIS; Santiago de Compostela, Spain) and was authorized under procedure number 15011/2021/002 by the Farming and Ranching Agency of Xunta de Galicia (Regional Government, Spain) in agreement with European (Council Directive 2010/63/UE) and Spanish regulations (RD 53/2013).

Supplementary material

Supplemental material for this article is available online.

Glossary

2k2c	two-kidney, two-clip
AQ4	aquaporin 4
BBB	blood-brain barrier
BP	blood pressures
cSVD	cerebral small vessel disease
FOV	field of view
IL	interleukin
INL	inner nuclear layers
MMP9	matrix metalloproteinase-9
MRI	magnetic resonance image
MSME	multi-slice multi-echo
ONL	inner nuclear layers
PFA	paraformaldehyde
RHRSP	stroke-prone renovascular hypertensive rat
SHRSP	stroke-prone spontaneously hypertensive rat
sTWEAK	soluble tumor necrosis factor-like weak inducer of apoptosis
TNF-α	tumor necrosis factor alpha
WML	white matter lesions

References

Armulik, A., Genové, G., Mäe, M., Nisancioglu, M.H., Wallgard, E., Niaudet, C., He, L., Norlin, J., Lindblom, P., Strittmatter, K., Johansson, B.R., Betsholtz, C., 2010. Pericytes regulate the blood–brain barrier. Nature 468, 557–561. https://doi.org/10.1038/nature09522

Bailey, E.L., Smith, C., Sudlow, C.L.M., Wardlaw, J.M., 2011. Is the Spontaneously Hypertensive Stroke Prone Rat a Pertinent Model of Sub Cortical Ischemic Stroke? A Systematic Review. Int. J. Stroke 6, 434–444. https://doi.org/10.1111/j.1747-4949.2011.00659.x

Blanco-Colio, L.M., Martín-Ventura, J.L., Muñóz-García, B., Orbe, J., Páramo, J.A., Michel, J.-B., Ortiz, A., Meilhac, O., Egido, J., 2007. Identification of Soluble Tumor Necrosis Factor-Like Weak Inducer of Apoptosis (sTWEAK) as a Possible Biomarker of Subclinical Atherosclerosis. Arterioscler. Thromb. Vasc. Biol. 27, 916–922. https://doi.org/10.1161/01.ATV.0000258972.10109.ff

Boehme, A.K., Esenwa, C., Elkind, M.S.V., 2017. Stroke Risk Factors, Genetics, and Prevention. Circ. Res. 120, 472–495. https://doi.org/10.1161/CIRCRESAHA.116.308398

Cannistraro, R.J., Badi, M., Eidelman, B.H., Dickson, D.W., Middlebrooks, E.H., Meschia, J.F., 2019. CNS small vessel disease. Neurology 92, 1146–1156. https://doi.org/10.1212/WNL.0000000000007654

Castillo, J., Leira, R., García, M.M., Serena, J., Blanco, M., Dávalos, A., 2004. Blood Pressure Decrease During the Acute Phase of Ischemic Stroke Is Associated With Brain Injury and Poor Stroke Outcome. Stroke 35, 520–526.

https://doi.org/10.1161/01.STR.0000109769.22917.B0

Chaganti, J., Zeng, G., Tun, N., Lockart, I., Abdelshaheed, C., Cysique, L., Montagnese, S., Brew, B.J., Danta, M., 2023. Novel magnetic resonance KTRANS measurement of blood-brain barrier permeability correlated with covert HE. Hepatol. Commun. 7, e0079. https://doi.org/10.1097/HC9.0000000000000079

Chen, X., Liao, S., Ye, L., Gong, Q., Ding, Q., Zeng, J., Yu, J., 2014. Neuroprotective effect of chondroitinase ABC on primary and secondary brain injury after stroke in hypertensive rats. Brain Res. 1543, 324–333. https://doi.org/10.1016/j.brainres.2013.12.002

Chorianopoulos, E., Jarr, K., Steen, H., Giannitsis, E., Frey, N., Katus, H.A., 2010. Soluble TWEAK is markedly upregulated in patients with ST-elevation myocardial infarction and related to an adverse short-term outcome. Atherosclerosis 211, 322–326. https://doi.org/10.1016/j.atherosclerosis.2010.02.016

Chorianopoulos, E., Rosenberg, M., Zugck, C., Wolf, J., Katus, H.A., Frey, N., 2009. Decreased soluble TWEAK levels predict an adverse prognosis in patients with chronic stable heart failure. Eur. J. Heart Fail. 11, 1050–1056. https://doi.org/10.1093/eurjhf/hfp139

Comertpay, E., Vural, S., Eroğlu, O., Dindar Badem, N., Bilgili, Y., Coskun, F., 2020. The diagnostic value of sTWEAK in acute ischemic stroke. Balkan Med. J. 37, 336–340. https://doi.org/10.4274/balkanmedj.galenos.2020.2020.2.45

Dai, J.-X., Cai, J.-Y., Sun, J., Lin, Q., Yu, Z.-Q., 2020. Serum soluble tumor necrosis factor-like weak inducer of apoptosis is a potential biomarker for outcome prediction of patients with aneurysmal subarachnoid hemorrhage. Clin. Chim. Acta 510, 354–

359. https://doi.org/10.1016/j.cca.2020.07.052

Del Bigio, M.R., Yan, H.J., Kozlowski, P., Sutherland, G.R., Peeling, J., 1999. Serial Magnetic Resonance Imaging of Rat Brain After Induction of Renal Hypertension. Stroke 30, 2440–2447. https://doi.org/10.1161/01.STR.30.11.2440

Duering, M., Biessels, G.J., Brodtmann, A., Chen, C., Cordonnier, C., de Leeuw, F.-E., Debette, S., Frayne, R., Jouvent, E., Rost, N.S., ter Telgte, A., Al-Shahi Salman, R., Backes, W.H., Bae, H.-J., Brown, R., Chabriat, H., De Luca, A., DeCarli, C., Dewenter, A., Doubal, F.N., Ewers, M., Field, T.S., Ganesh, A., Greenberg, S., Helmer, K.G., Hilal, S., Jochems, A.C.C., Jokinen, H., Kuijf, H., Lam, B.Y.K., Lebenberg, J., MacIntosh, B.J., Maillard, P., Mok, V.C.T., Pantoni, L., Rudilosso, S., Satizabal, C.L., Schirmer, M.D., Schmidt, R., Smith, C., Staals, J., Thrippleton, M.J., van Veluw, S.J., Vemuri, P., Wang, Y., Werring, D., Zedde, M., Akinyemi, R.O., Del Brutto, O.H., Markus, H.S., Zhu, Y.-C., Smith, E.E., Dichgans, M., Wardlaw, J.M., 2023. Neuroimaging standards for research into small vessel disease—advances since 2013. Lancet Neurol. 22, 602–618. https://doi.org/10.1016/S1474-4422(23)00131-X

Dunlay, S.M., Weston, S.A., Redfield, M.M., Killian, J.M., Roger, V.L., 2008. Tumor Necrosis Factor-α and Mortality in Heart Failure. Circulation 118, 625–631. https://doi.org/10.1161/CIRCULATIONAHA.107.759191

Durukan, A., Marinkovic, I., Strbian, D., Pitkonen, M., Pedrono, E., Soinne, L., Abo-Ramadan, U., Tatlisumak, T., 2009. Post-ischemic blood–brain barrier leakage in rats: One-week follow-up by MRI. Brain Res. 1280, 158–165. https://doi.org/10.1016/j.brainres.2009.05.025

Dziedziak, J., Zaleska-Żmijewska, A., Szaflik, J.P., Cudnoch-Jędrzejewska, A., 2022. Impact of Arterial Hypertension on the Eye: A Review of the Pathogenesis, Diagnostic Methods, and Treatment of Hypertensive Retinopathy. Med. Sci. Monit. 28, e935135. https://doi.org/10.12659/MSM.935135

Elsaid, N., Saied, A., Kandil, H., Soliman, A., Taher, F., Hadi, M., Giridharan, G., Jennings, R., Casanova, M., Keynton, R., El-Baz, A., 2021. Impact of stress and hypertension on the cerebrovasculature. Front. Biosci. 26, 1643–1652. https://doi.org/10.52586/5057

Fan, Y., Lan, L., Zheng, L., Ji, X., Lin, J., Zeng, J., Huang, R., Sun, J., 2015a. Spontaneous white matter lesion in brain of stroke-prone renovascular hypertensive rats: a study from MRI, pathology and behavior. Metab. Brain Dis. 30, 1479–1486. https://doi.org/10.1007/s11011-015-9722-9

Fan, Y., Yang, X., Tao, Y., Lan, L., Zheng, L., Sun, J., 2015b. Tight junction disruption of blood–brain barrier in white matter lesions in chronic hypertensive rats. Neuroreport 26, 1039–1043. https://doi.org/10.1097/WNR.0000000000000464

Fernandez-Bueno, I., Alonso-Alonso, M.-L., Garcia-Gutierrez, M.-T., Diebold, Y., 2019. Reliability and reproducibility of a rodent model of choroidal neovascularization based on the subretinal injection of polyethylene glycol. Mol. Vis. 25, 194–203.

Fernandez-Bueno, I., Jones, R., Soriano-Romaní, L., López-García, A., Galvin, O., Cheetham, S., Diebold, Y., 2017. Histologic Characterization of Retina Neuroglia Modifications in Diabetic Zucker Diabetic Fatty Rats. Investig. Opthalmology Vis. Sci. 58, 4925–4933. https://doi.org/10.1167/iovs.17-21742

Fernández-Laso, V., Sastre, C., Valdivielso, J.M., Fernández, E., Martín-Ventura, J.L.,

Egido, J., Blanco-Colio, L.M., 2015. Soluble TWEAK levels predict the presence of carotid atherosclerotic plaques in subjects free from clinical cardiovascular diseases. Atherosclerosis 239, 358–363. https://doi.org/10.1016/j.atherosclerosis.2015.01.040

Fuchs, F.D., Whelton, P.K., 2020. High Blood Pressure and Cardiovascular Disease. Hypertension 75, 285–292. https://doi.org/10.1161/HYPERTENSIONAHA.119.14240

Fukuda, A.M., Badaut, J., 2012. Aquaporin 4: a player in cerebral edema and neuroinflammation. J. Neuroinflammation 9, 279. https://doi.org/10.1186/1742-2094-9-279

Girach, Z., Sarian, A., Maldonado-García, C., Ravikumar, N., Sergouniotis, P.I., Rothwell, P.M., Frangi, A.F., Julian, T.H., 2024. Retinal imaging for the assessment of stroke risk: a systematic review. J. Neurol. 271, 2285–2297. https://doi.org/10.1007/s00415-023-12171-6

Gröhn, O.H.J., Lukkarinen, J.A., Oja, J.M.E., van Zijl, P.C.M., Ulatowski, J.A., Traystman, R.J., Kauppinen, R.A., 1998. Noninvasive Detection of Cerebral Hypoperfusion and Reversible Ischemia from Reductions in the Magnetic Resonance Imaging Relaxation Time, T 2. J. Cereb. Blood Flow Metab. 18, 911–920. https://doi.org/10.1097/00004647-199808000-00012

Hainsworth, A.H., Markus, H.S., 2008. Do in vivo Experimental Models Reflect Human Cerebral Small Vessel Disease? a Systematic Review. J. Cereb. Blood Flow Metab. 28, 1877–1891. https://doi.org/10.1038/jcbfm.2008.91

Hainsworth, A.H., Markus, H.S., Schneider, J.A., 2024. Cerebral Small Vessel Disease,

Hypertension, and Vascular Contributions to Cognitive Impairment and Dementia. Hypertension 81, 75–86. https://doi.org/10.1161/HYPERTENSIONAHA.123.19943

Hannawi, Y., 2024. Cerebral Small Vessel Disease: a Review of the Pathophysiological Mechanisms. Transl. Stroke Res. 15, 1050–1069. https://doi.org/10.1007/s12975-023-01195-9

Herman, I.M., Jacobson, S., 1988. In situ analysis of microvascular pericytes in hypertensive rat brains. Tissue Cell 20, 1–12. https://doi.org/10.1016/0040-8166(88)90002-X

Hervella, P., Pérez-Mato, M., Rodríguez-Yáñez, M., López-Dequidt, I., Pumar, J.M., Sobrino, T., Campos, F., Castillo, J., da Silva-Candal, A., Iglesias-Rey, R., 2021. sTWEAK as Predictor of Stroke Recurrence in Ischemic Stroke Patients Treated With Reperfusion Therapies. Front. Neurol. 12, 652867. https://doi.org/10.3389/fneur.2021.652867

Hervella, P., Sampedro-Viana, A., Rodríguez-Yáñez, M., López-Dequidt, I., Pumar, J.M., Mosqueira, A.J., Fernández-Rodicio, S., Bazarra-Barreiros, M., Serena, J., Silva-Blas, Y., Gubern-Merida, C., Rey-Aldana, D., Cinza, S., Campos, F., Sobrino, T., Castillo, J., Alonso-Alonso, M.L., Iglesias-Rey, R., 2024. Systemic biomarker associated with poor outcome after futile reperfusion. Eur. J. Clin. Invest. 54, 1–11. https://doi.org/10.1111/eci.14181

Higashi, Y., 2023. Smoking cessation and vascular endothelial function. Hypertens. Res. 46, 2670–2678. https://doi.org/10.1038/s41440-023-01455-z

Huang, J., Li, J., Feng, C., Huang, X., Wong, L., Liu, X., Nie, Z., Xi, G., 2018. Blood-Brain Barrier Damage as the Starting Point of Leukoaraiosis Caused by Cerebral Chronic

Hypoperfusion and Its Involved Mechanisms: Effect of Agrin and Aquaporin-4. Biomed Res. Int. 2018, 1–10. https://doi.org/10.1155/2018/2321797

Iglesias-Rey, R., Custodia, A., Alonso-Alonso, M.L., López-Dequidt, I., Rodríguez-Yáñez, M., Pumar, J.M., Castillo, J., Sobrino, T., Campos, F., Silva-Candal, A. da, Hervella, P., 2022. The Smoking Paradox in Stroke Patients Under Reperfusion Treatment Is Associated With Endothelial Dysfunction. Front. Neurol. 13, 841484. https://doi.org/10.3389/fneur.2022.841484

Ihara, M., Yamamoto, Y., 2016. Emerging Evidence for Pathogenesis of Sporadic Cerebral Small Vessel Disease. Stroke 47, 554–560. https://doi.org/10.1161/STROKEAHA.115.009627

Lan, L.L.-F., Zheng, L., Yang, X., Ji, X.X.-T., Fan, Y.Y.-H., Zeng, J.-S.J., 2015. Peroxisome Proliferator-activated Receptor-γ Agonist Pioglitazone Ameliorates White Matter Lesion and Cognitive Impairment in Hypertensive Rats. CNS Neurosci. Ther. 21, 410–416. https://doi.org/10.1111/cns.12374

Leira, R., Millán, M., Díez-Tejedor, E., Blanco, M., Serena, J., Fuentes, B., Rodríguez-Yáñez, M., Castellanos, M., Lago, A., Dávalos, A., Castillo, J., 2009. Age Determines the Effects of Blood Pressure Lowering During the Acute Phase of Ischemic Stroke. Hypertension 54, 769–774. https://doi.org/10.1161/HYPERTENSIONAHA.109.133546

Li, M., Zhao, Y., Hao, H., Dai, H., Han, Q., Tong, C., Liu, J., Han, W., Fu, X., 2015. Mesenchymal stem cell-conditioned medium improves the proliferation and migration of keratinocytes in a diabetes-like microenvironment. Int. J. Low. Extrem. Wounds 14, 73–86. https://doi.org/10.1177/1534734615569053

Li, Y., Wang, Q., Muir, E.R., Kiel, J.W., Duong, T.Q., 2020. Retinal Vascular and Anatomical Features in the Spontaneously Hypertensive Rat. Curr. Eye Res. 45, 1422–1429. https://doi.org/10.1080/02713683.2020.1752738

Liang, Y., Liu, B., Xiao, Y., Zeng, X., Wu, G., Du, Z., Fang, Y., Hu, Y., Yang, X., Yu, H., 2022. Retinal Neurovascular Changes in Patients With Ischemic Stroke Investigated by Optical Coherence Tomography Angiography. Front. Aging Neurosci. 14. https://doi.org/10.3389/fnagi.2022.834560

Lin, J., Lan, L., Wang, D., Qiu, B., Fan, Y., 2017a. Cerebral Venous Collagen Remodeling in a Modified White Matter Lesions Animal Model. Neuroscience 367, 72–84. https://doi.org/10.1016/j.neuroscience.2017.10.031

Lin, J., Wang, D., Lan, L., Fan, Y., 2017b. Multiple Factors Involved in the Pathogenesis of White Matter Lesions. Biomed Res. Int. 2017, 1–9. https://doi.org/10.1155/2017/9372050

Ling, L., Zeng, J., Pei, Z., Cheung, R.T., Hou, Q., Xing, S., Zhang, S., 2009. Neurogenesis and Angiogenesis within the Ipsilateral Thalamus with Secondary Damage after Focal Cortical Infarction in Hypertensive Rats. J. Cereb. Blood Flow Metab. 29, 1538–1546. https://doi.org/10.1038/jcbfm.2009.76

Liu, C.-L., Liao, S.-J., Zeng, J.-S., Lin, J.-W., Li, C.-X., Xie, L.-C., Shi, X.-G., Huang, R.-X., 2007. dl-3n-butylphthalide prevents stroke via improvement of cerebral microvessels in RHRSP. J. Neurol. Sci. 260, 106–113. https://doi.org/10.1016/j.jns.2007.04.025

Mader, S., Brimberg, L., 2019. Aquaporin-4 Water Channel in the Brain and Its Implication for Health and Disease. Cells 8, 90.

https://doi.org/10.3390/cells8020090

Markus, H.S., de Leeuw, F.E., 2023. Cerebral small vessel disease: Recent advances and future directions. Int. J. Stroke 18, 4–14. https://doi.org/10.1177/17474930221144911

Martín-Ventura, J.L., Muñóz-García, B., Egido, J., Blanco-Colio, L.M., 2010. TWEAK soluble, un nuevo biomarcador de riesgo cardiovascular. Clínica e Investig. en Arterioscler. 22, 99–104. https://doi.org/10.1016/j.arteri.2009.09.001

Meissner, A., 2016. Hypertension and the Brain: A Risk Factor for More Than Heart Disease. Cerebrovasc. Dis. 42, 255–262. https://doi.org/10.1159/000446082

Meschia, J.F., Bushnell, C., Boden-Albala, B., Braun, L.T., Bravata, D.M., Chaturvedi, S., Creager, M.A., Eckel, R.H., Elkind, M.S. V, Fornage, M., Goldstein, L.B., Greenberg, S.M., Horvath, S.E., Iadecola, C., Jauch, E.C., Moore, W.S., Wilson, J.A., American Heart Association Stroke Council, Council on Cardiovascular and Stroke Nursing, Council on Clinical Cardiology, Council on Functional Genomics and Translational Biology, Council on Hypertension, 2014. Guidelines for the primary prevention of stroke: a statement for healthcare professionals from the American Heart Association/American Stroke Association. Stroke 45, 3754–3832. https://doi.org/10.1161/STR.0000000000000046

Montellano, F.A., Ungethüm, K., Ramiro, L., Nacu, A., Hellwig, S., Fluri, F., Whiteley, W.N., Bustamante, A., Montaner, J., Heuschmann, P.U., 2021. Role of Blood-Based Biomarkers in Ischemic Stroke Prognosis. Stroke 52, 543–551. https://doi.org/10.1161/STROKEAHA.120.029232

Morgan, C.A., Mesquita, M., Ashioti, M., Beech, J.S., Williams, S.C.R., Irving, E., Cash,

D., 2020. Late changes in blood–brain barrier permeability in a rat tMCAO model of stroke detected by gadolinium-enhanced MRI. Neurol. Res. 42, 844–852. https://doi.org/10.1080/01616412.2020.1786637

Mueller, S.M., Heistad, D.D., 1980. Effect of chronic hypertension on the blood-brain barrier. Hypertension 2, 809–812. https://doi.org/10.1161/01.HYP.2.6.809

Mustapha, M., Nassir, C.M.N.C.M., Aminuddin, N., Safri, A.A., Ghazali, M.M., 2019. Cerebral Small Vessel Disease (CSVD) – Lessons From the Animal Models. Front. Physiol. 10, 1317. https://doi.org/10.3389/fphys.2019.01317

Nabika, T., Cui, Z., Masuda, J., 2004. The Stroke-Prone Spontaneously Hypertensive Rat: How Good Is It as a Model for Cerebrovascular Diseases? Cell. Mol. Neurobiol. 24, 639–646. https://doi.org/10.1023/B:CEMN.0000036402.79129.2f

NCD Risk Factor Collaboration (NCD-RisC)., 2021. Worldwide trends in hypertension prevalence and progress in treatment and control from 1990 to 2019: a pooled analysis of 1201 population-representative studies with 104 million participants. Lancet 398, 957–980. https://doi.org/10.1016/S0140-6736(21)01330-1

O'Sullivan, M., 2008. Leukoaraiosis. Pract. Neurol. 8, 26–38. https://doi.org/10.1136/jnnp.2007.139428

Okamoto, K., Yamori, Y., Nagaoka, A., 1974. Establishment of the stroke prone spontaneously hypertensive rat (SHR). Circ. Res. 34, I143–I153.

On, N.H., Mitchell, R., Savant, S.D., Bachmeier, C.J., Hatch, G.M., Miller, D.W., 2013. Examination of blood–brain barrier (BBB) integrity in a mouse brain tumor model. J. Neurooncol. 111, 133–143. https://doi.org/10.1007/s11060-012-1006-1

Ong, Y.-T., Wong, T.Y., Klein, R., Klein, B.E.K., Mitchell, P., Sharrett, A.R., Couper, D.J., Ikram, M.K., 2013. Hypertensive Retinopathy and Risk of Stroke. Hypertension 62, 706–711. https://doi.org/10.1161/HYPERTENSIONAHA.113.01414

Park, H., Park, J.H., Lee, S.J., 2016. In vivo measurement of hemodynamic information in stenosed rat blood vessels using X-ray PIV. Sci. Rep. 6, 37985. https://doi.org/10.1038/srep37985

Rodríguez, I., Lema, I., Blanco, M., Rodríguez-Yáñez, M., Leira, R., Castillo, J., 2010. Vascular Retinal, Neuroimaging and Ultrasonographic Markers of Lacunar Infarcts. Int. J. Stroke 5, 360–366. https://doi.org/10.1111/j.1747-4949.2010.00462.x

Schindelin, J., Arganda-Carreras, I., Frise, E., Kaynig, V., Longair, M., Pietzsch, T., Preibisch, S., Rueden, C., Saalfeld, S., Schmid, B., Tinevez, J.-Y., White, D.J., Hartenstein, V., Eliceiri, K., Tomancak, P., Cardona, A., 2012. Fiji: an open-source platform for biological-image analysis. Nat. Methods 9, 676–682. https://doi.org/10.1038/nmeth.2019

Shindo, A., Ishikawa, H., Ii, Y., Niwa, A., Tomimoto, H., 2020. Clinical Features and Experimental Models of Cerebral Small Vessel Disease. Front. Aging Neurosci. 12, 109. https://doi.org/10.3389/fnagi.2020.00109

Simpson, J.E., Wharton, S.B., Cooper, J., Gelsthorpe, C., Baxter, L., Forster, G., Shaw, P.J., Savva, G., Matthews, F.E., Brayne, C., Ince, P.G., 2010. Alterations of the blood–brain barrier in cerebral white matter lesions in the ageing brain. Neurosci. Lett. 486, 246–251. https://doi.org/10.1016/j.neulet.2010.09.063

Strbian, D., Durukan, A., Pitkonen, M., Marinkovic, I., Tatlisumak, E., Pedrono, E., Abo-Ramadan, U., Tatlisumak, T., 2008. The blood-brain barrier is continuously open

for several weeks following transient focal cerebral ischemia. Neuroscience 153, 175–181. https://doi.org/10.1016/j.neuroscience.2008.02.012

Tamaki, K., Sadoshima, S., Baumbach, G.L., Iadecola, C., Reis, D.J., Heistad, D.D., 1984. Evidence that disruption of the blood-brain barrier precedes reduction in cerebral blood flow in hypertensive encephalopathy. Hypertens. (Dallas, Tex. 1979) 6, I75-81. https://doi.org/10.1161/01.hyp.6.2_pt_2.i75

Tomassoni, D., Bramanti, V., Amenta, F., 2010. Expression of aquaporins 1 and 4 in the brain of spontaneously hypertensive rats. Brain Res. 1325, 155–163. https://doi.org/10.1016/j.brainres.2010.02.023

van Vliet, E.A., Ndode-Ekane, X.E., Lehto, L.J., Gorter, J.A., Andrade, P., Aronica, E., Gröhn, O., Pitkänen, A., 2020. Long-lasting blood-brain barrier dysfunction and neuroinflammation after traumatic brain injury. Neurobiol. Dis. 145, 105080. https://doi.org/10.1016/j.nbd.2020.105080

van Vliet, E.A., Otte, W.M., Gorter, J.A., Dijkhuizen, R.M., Wadman, W.J., 2014. Longitudinal assessment of blood–brain barrier leakage during epileptogenesis in rats. A quantitative MRI study. Neurobiol. Dis. 63, 74–84. https://doi.org/10.1016/j.nbd.2013.11.019

van Vliet, E.A., Otte, W.M., Wadman, W.J., Aronica, E., Kooij, G., de Vries, H.E., Dijkhuizen, R.M., Gorter, J.A., 2016. Blood–brain barrier leakage after status epilepticus in rapamycin-treated rats I: Magnetic resonance imaging. Epilepsia 57, 59–69. https://doi.org/10.1111/epi.13246

Verkman, A.S., 2013. Aquaporins. Curr. Biol. 23, R52–R55. https://doi.org/10.1016/j.cub.2012.11.025

Wajngarten, M., Silva, G.S., 2019. Hypertension and Stroke: Update on Treatment. Eur. Cardiol. Rev. 14, 111–115. https://doi.org/10.15420/ecr.2019.11.1

Wardlaw, J.M., Smith, C., Dichgans, M., 2019. Small vessel disease: mechanisms and clinical implications. Lancet Neurol. 18, 684–696. https://doi.org/10.1016/S1474-4422(19)30079-1

Wei, W., Ma, D., Li, L., Zhang, L., 2024. Cognitive impairment in cerebral small vessel disease induced by hypertension. Neural Regen. Res. 19, 1454–1462. https://doi.org/10.4103/1673-5374.385841

Wu, H.-Q., Wu, H., Shi, L.-L., Yu, L.-Y., Wang, L.-Y., Chen, Y.-L., Geng, J.-S., Shi, J., Jiang, K., Dong, J.-C., 2017. The association between retinal vasculature changes and stroke: a literature review and Meta-analysis. Int. J. Ophthalmol. 10, 109–114. https://doi.org/10.18240/ijo.2017.01.18

Xu, X., Xiao, C., Yi, M., Yang, J., Liao, M., Zhou, K., Hu, L., Ouyang, F., Lan, L., Fan, Y., 2024. Cerebral Perfusion Characteristics and Dynamic Brain Structural Changes in Stroke-Prone Renovascular Hypertensive Rats: A Preclinical Model for Cerebral Small Vessel Disease. Transl. Stroke Res. https://doi.org/10.1007/s12975-024-01239-8

Xue, Y., Zeng, X., Tu, W.-J., Zhao, J., 2022. Tumor Necrosis Factor-α: The Next Marker of Stroke. Dis. Markers 2022, 1–8. https://doi.org/10.1155/2022/2395269

Yepes, M., 2013. TWEAK and Fn14 in the Neurovascular Unit. Front. Immunol. 4, 367. https://doi.org/10.3389/fimmu.2013.00367

Yepes, M., 2007. TWEAK and the Central Nervous System. Mol. Neurobiol. 35, 255–

265. https://doi.org/10.1007/s12035-007-0024-z

Ying, Y., Li, Y., Yao, T., Shao, X., Tang, W., Montagne, A., Chabriat, H., Wang, D.J.J., Wang, C., Yang, Q., Cheng, X., 2024. Heterogeneous blood-brain barrier dysfunction in cerebral small vessel diseases. Alzheimer's Dement. 20, 4527–4539. https://doi.org/10.1002/alz.13874

Zeng, J., Zhang, Y., Mo, J., Su, Z., Huang, R., 1998. Two-Kidney, Two Clip Renovascular Hypertensive Rats Can Be Used as Stroke-prone Rats. Stroke 29, 1708–1714. https://doi.org/10.1161/01.STR.29.8.1708

Zhang, B., Zhang, Y., Deng, F., Fang, S., 2020. Ligustrazine prevents basilar artery remodeling in two-kidney-two-clip renovascular hypertension rats via suppressing PI3K/Akt signaling. Microvasc. Res. 128, 103938. https://doi.org/10.1016/j.mvr.2019.103938

Figure captations

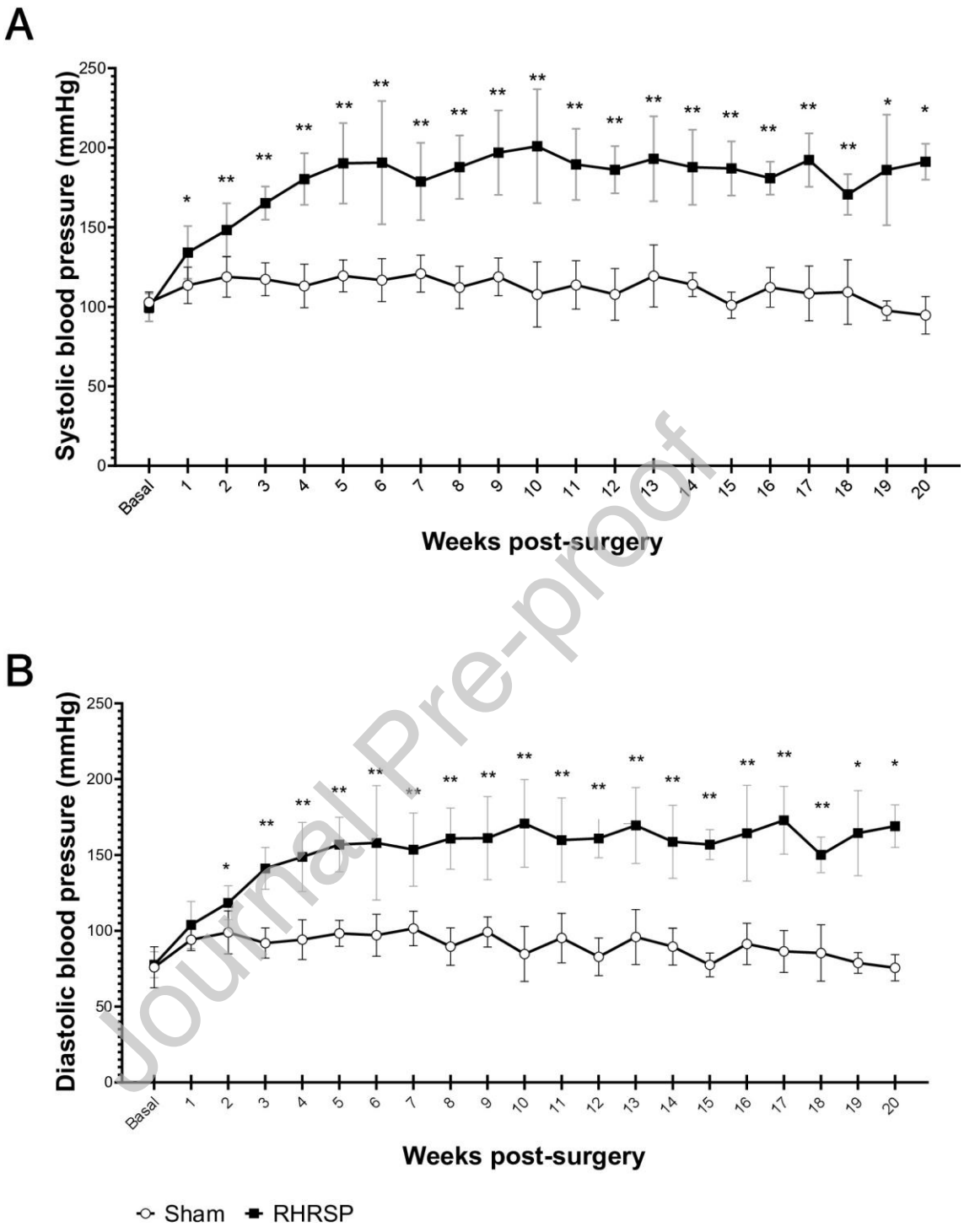

Fig. 1. Blood pressure after implantation of the arterial stenosis clips both renal arteries. It was observed that the systolic blood pressure (A) of the rats with the device was significantly higher since the first post-surgical week. This significant difference was also observed in the case of diastolic blood pressure (B) since the second week post-surgery.

Sham (n=6) and RHRSP (n=6; weeks 16-18 n=5; weeks 19-20 n=4). RHRSP, stroke-prone renovascular hypertensive rats. Media ± SD; * p<0.05, ** p<0.001.

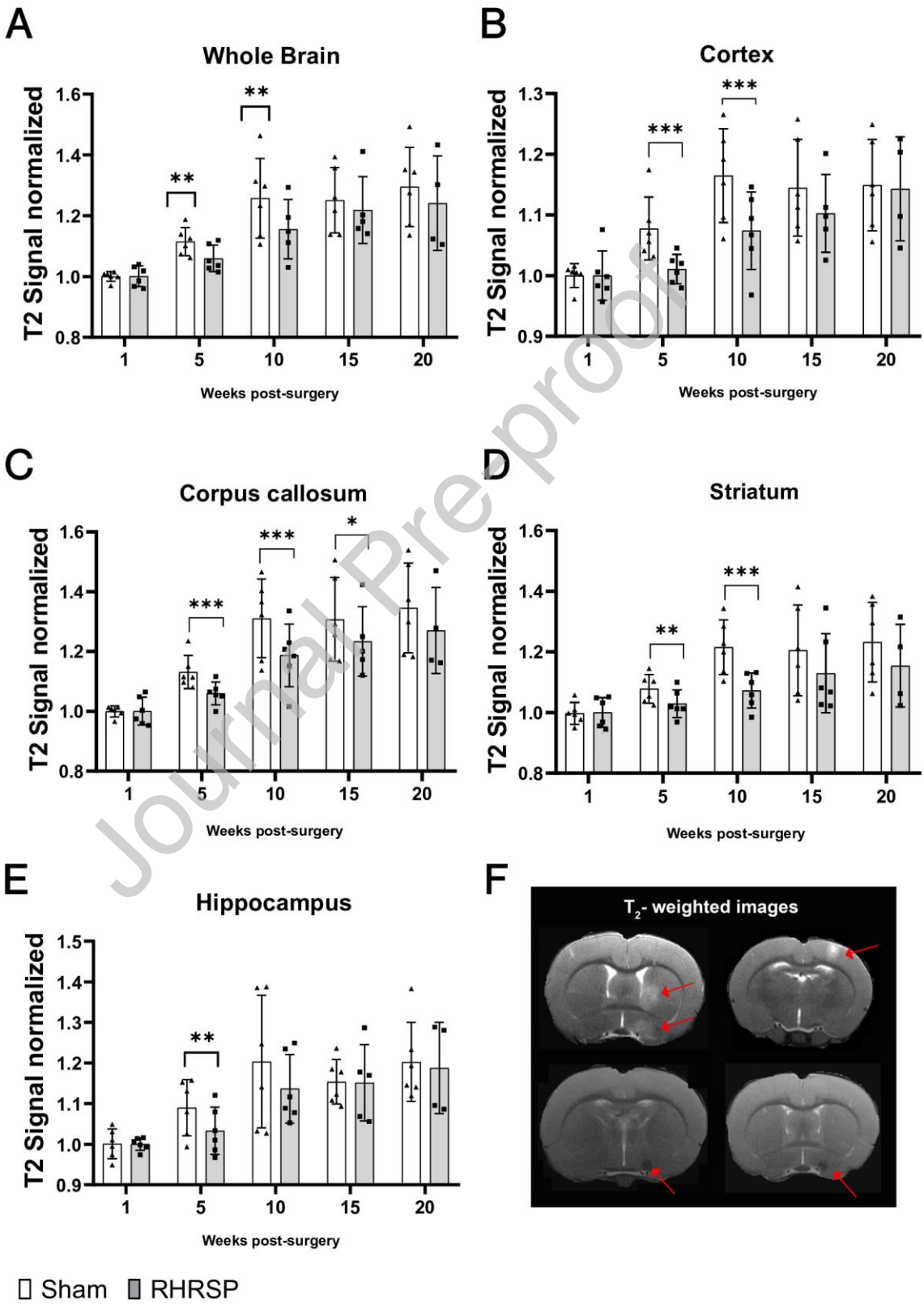

Fig. 2. T_2 signal normalized median values and brain lesions in MRI T_2-maps. T_2 signal normalized was lower in the RHRSP group in the whole brain (A), cortex (B), corpus callosum (C), striatum (D), and hippocampus (E). Brain lesions in T_2-weighted images correspond to the average of echoes 4 to 8 from the MSME sequence (F); arrows: ischemic lesions in top MRI and hemorrhage in bottom MRI. Sham (n=6) and RHRSP (n=6; week 15 n=5; week 20 n=4). RHRSP, stroke-prone renovascular hypertensive rats. Media ± SD; * $p<0.05$, ** $p<0.01$, *** $p<0.001$.

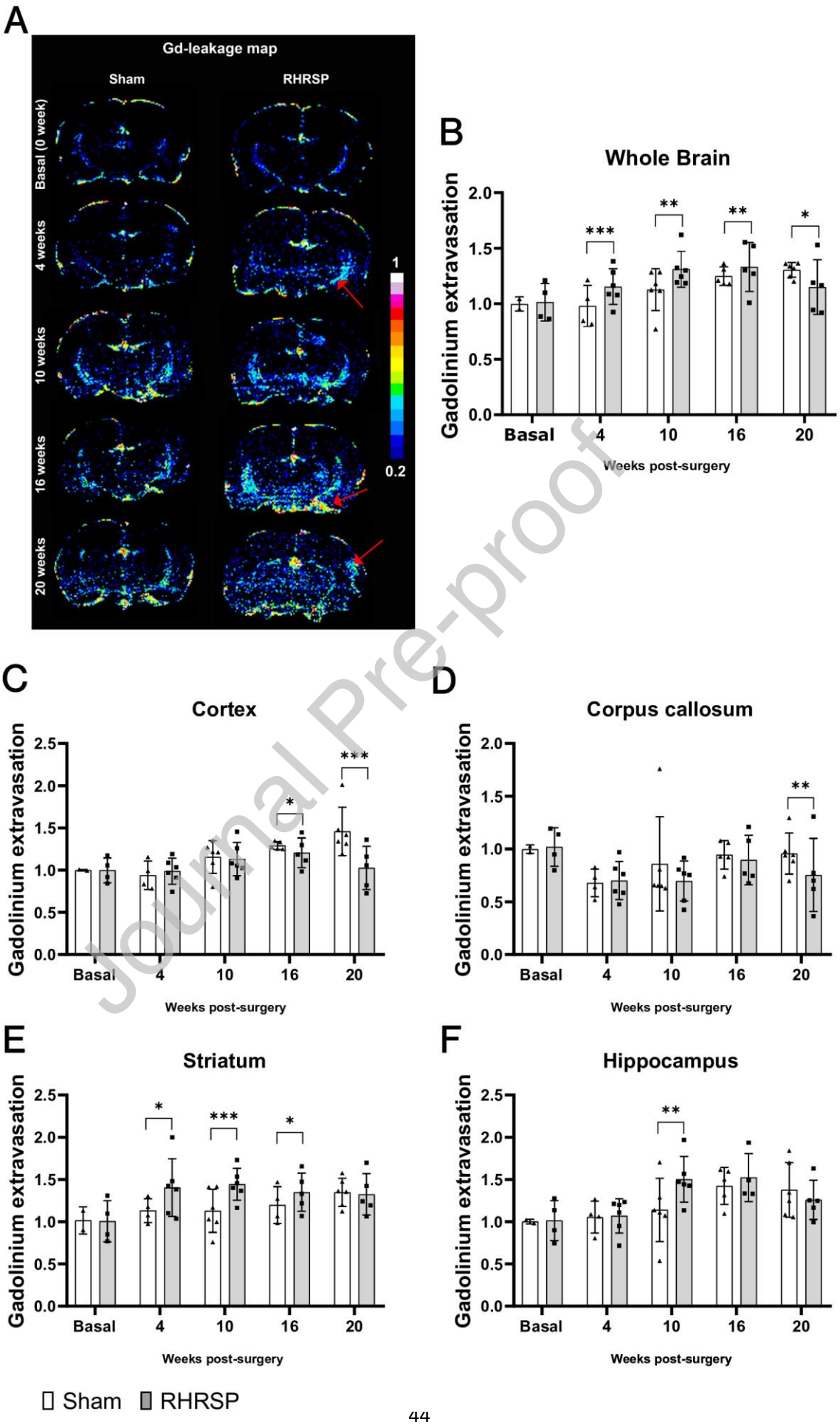

Fig. 3. Quantification of Gd-leakage after hypertension induction. Gd-leakage map (A). Normalized Gd-leakage measured in T_1-weighted MRI was performed to measure Gd extravasation in the whole brain (B), cortex (C), corpus callosum (D), striatum (E), and hippocampus (F). Sham (n=6) and RHRSP (n=6; week 15 n=5; weeks 20 n=4). Gd, gadolinium; RHRSP, stroke-prone renovascular hypertensive rats. Media ± SD; * p<0.05, ** p<0.01, *** p<0.001.

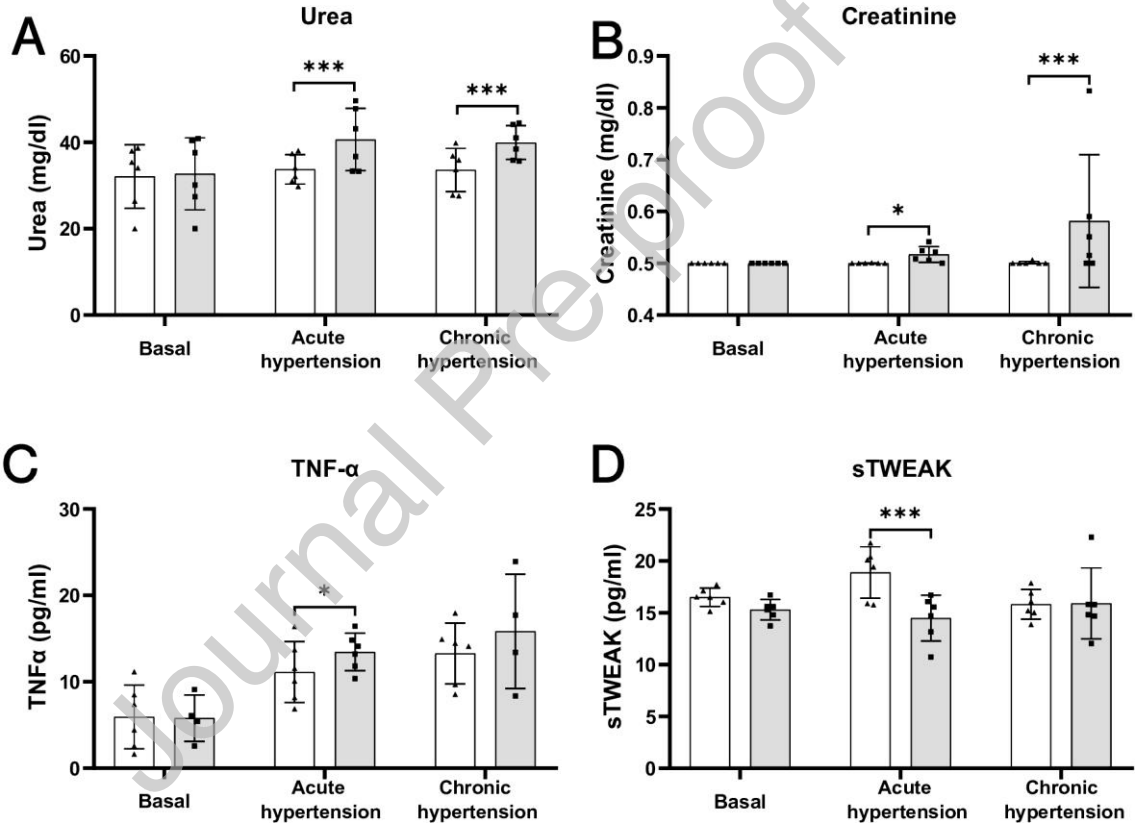

Fig. 4. Blood biomarkers. Urea (A) and creatinine (B) levels were used as renal function markers. Both were significantly increased in the RHRSP group after hypertension induction. Levels of TNF-α (C) were significantly increased during the acute hypertension phase. Conversely, sTWEAK levels (D) were significantly reduced during the acute hypertension phase. Acute hypertension (weeks 4, 8 & 12) and chronic hypertension

(weeks 16 &20); sham (n=6) and RHRSP (n=6; TNF-α n=4). sTWEAK, soluble tumor necrosis factor-like weak inducer of apoptosis; TNF-α, tumor necrosis factor alpha; RHRSP, stroke-prone renovascular hypertensive rats. Media ± SD; * p<0.05, *** p<0.001.

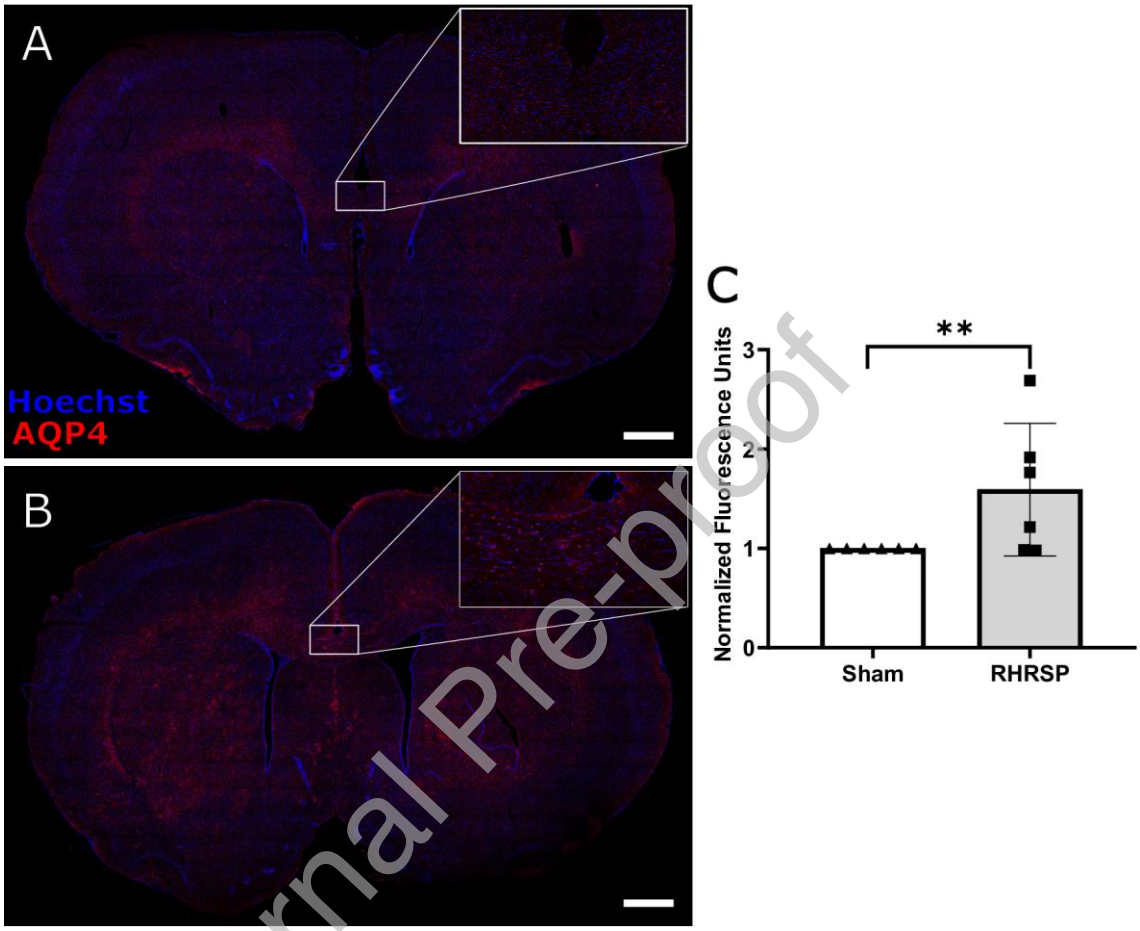

Fig. 5. AQP4 immunoreactivity in brain sections. AQP4 immunofluorescence in representative brain samples from sham (A) and RHRSP (B) rats. Immunoreactivity semiquantitation in duplicate (n=2 sections/rat) (C) showed a significant increment in AQP4 levels in the RHRSP group. Sham (n=6) and RHRSP (n=6). AQP4, aquaporin 4; RHRSP, stroke-prone renovascular hypertensive rats. Media ± SD; ** p<0.01. The scale bar denotes 1000 µm.

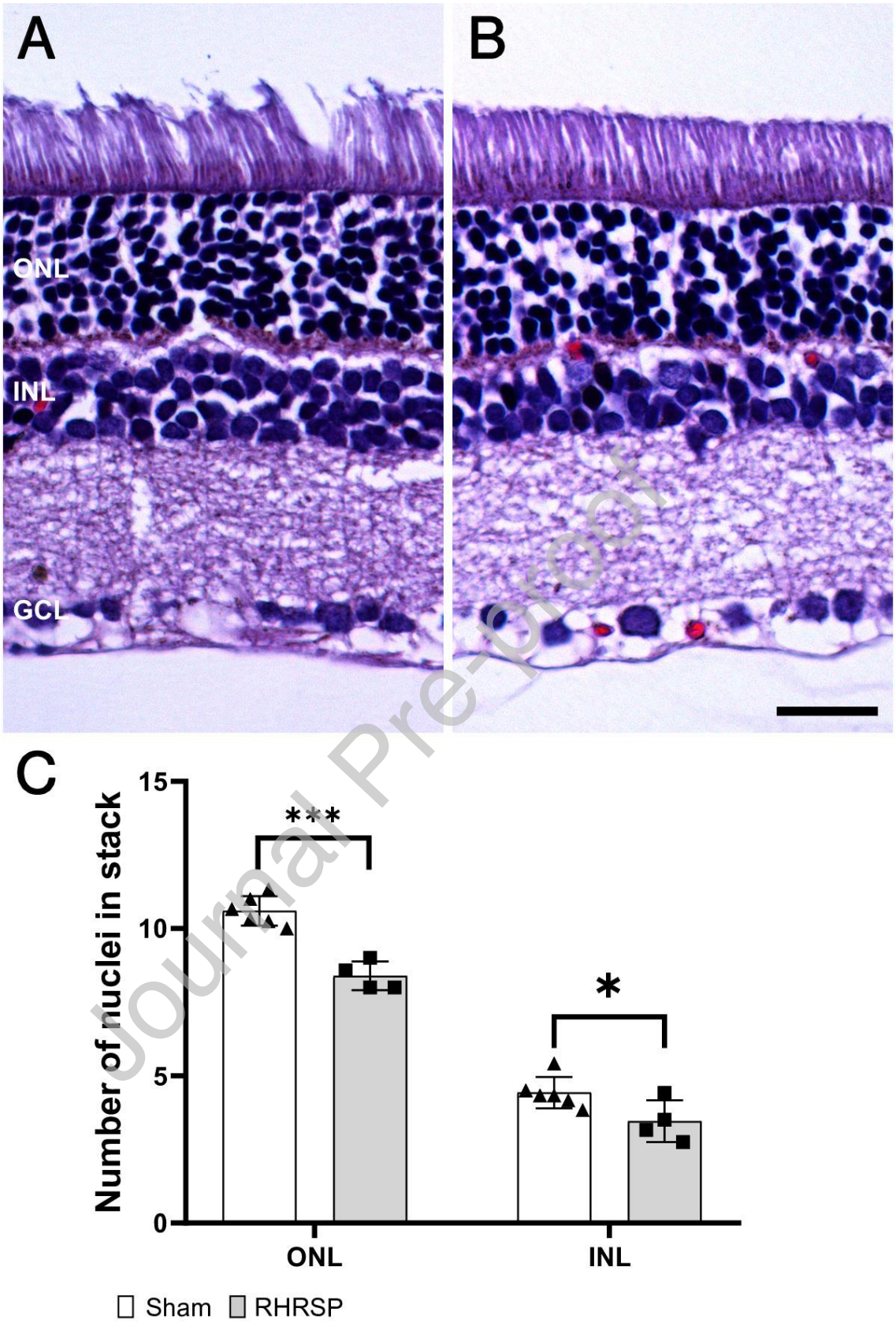

Fig. 6. Retinal general morphology and cell counts. Both sham (A) and RHRSP (B) rat retinas showed the typical highly organized layered structure with cells regularly

arranged (C). Number of nuclei per stack in the ONL and INL was significantly decreased in RHRSP rats. Sham (n=6) and RHRSP (n=4). Nucleus quantifications in triplicate (n=3 sections/rat) were performed. ONL, outer nuclear layer; INL inner nuclear layer; RHRSP, stroke-prone renovascular hypertensive rats. Media ± SD; * p<0.05, *** p<0.001. The scale bar denotes 50 µm.

Data Availability

Data will be made available on request.

Graphical Abstract

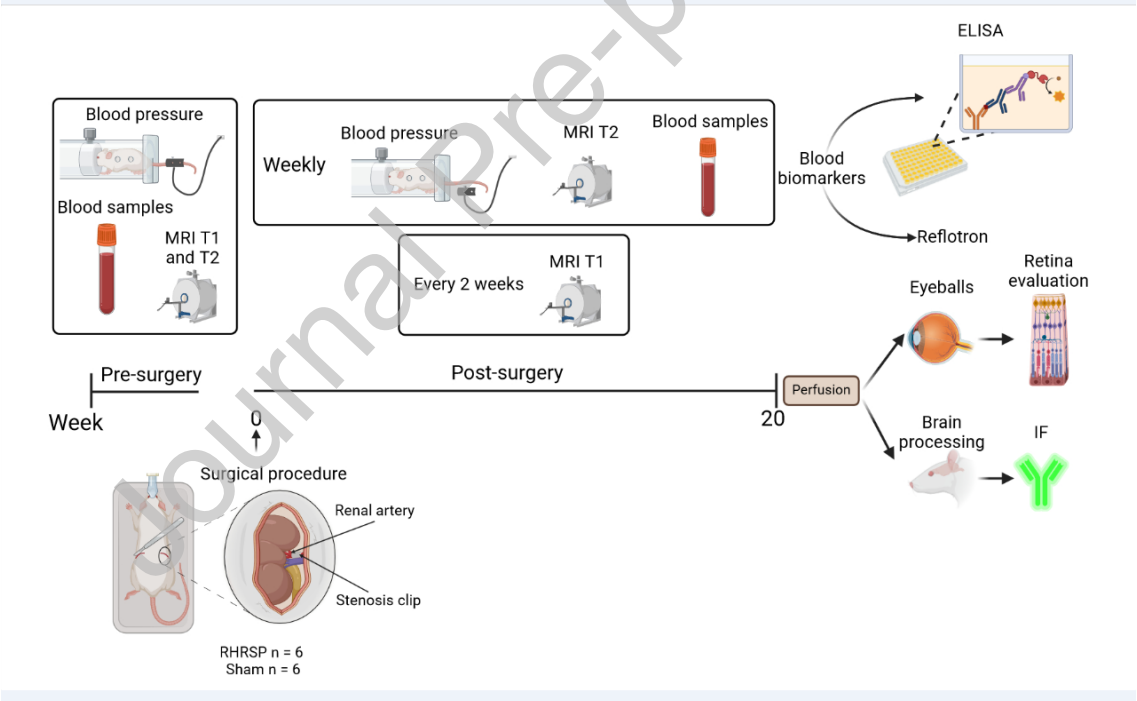

Declaration of interests

☒The authors declare that they have no known competing financial interests or personal relationships that could have appeared to influence the work reported in this paper.

☐The authors declare the following financial interests/personal relationships which may be considered as potential competing interests: